

# Synthesis of hierarchical three-dimensional CuO spindles for highly sensitive glucose determination

Ying Liu<sup>1</sup>, Qian Zhao<sup>1</sup>, Jieting Ding<sup>1</sup>, Hui Wang<sup>1</sup>, Yuanyuan Ma<sup>1</sup>, Weizhong Lv<sup>2</sup>, Shan Ji<sup>1,2</sup> ✉, Shunxi Li<sup>1</sup>, Rongfang Wang<sup>1</sup>

<sup>1</sup>Key Laboratory of Eco-Environment-Related Polymer Materials, Ministry of Education of China, College of Chemistry and Chemical Engineering, Northwest Normal University, Lanzhou 730070, People's Republic of China

<sup>2</sup>College of Chemistry and Chemical Engineering, Shenzhen University, Shenzhen 518060, People's Republic of China

✉ E-mail: jissshan@126.com

Published in *Micro & Nano Letters*; Received on 19th July 2016; Revised on 8th September 2016; Accepted on 13th September 2016

Hierarchical three-dimensional copper oxide (CuO) spindles were prepared via a hydrothermal process. The as-prepared CuO spindles assembled from nanoslices were characterised by scanning electron microscopy and transmission electron microscopy. The obtained hierarchical structure exhibited numerous particle boundaries acting as active sites for glucose oxidation in an alkaline solution. Chronoamperometric studies showed that under an optimal applied potential of +0.5 V versus Ag/AgCl, the as-prepared CuO electrode exhibited a broad detection range from 0.001 to 3.0 mM with a sensitivity of ca. 3000  $\mu\text{A mM}^{-1} \text{cm}^{-2}$  and a low detection limit of 0.3  $\mu\text{M}$ . The CuO spindle electrode also demonstrated excellent selectivity to glucose oxidation in the presence of several electro-active species.

**1. Introduction:** Sensing devices for rapid and accurate detection of glucose are required in areas of clinical diagnostics, biotechnology and food companies [1–3]. In the last decades, enzyme-based electrochemical biosensors have been widely used in glucose detection owing to their simple instrumentation, convenient operation, high sensitivity and good selectivity [4]. However, they possess many disadvantages, namely difficult immobilisation techniques, complicated operating conditions since glucose oxidase activity can be easily influenced by temperature, pH, chemicals, humidity, ionic detergents and other types of interference [5]. As an alternative strategy, the enzyme-free glucose sensors attracted considerable attentions since they offer many advantages over enzyme electrodes, such as low cost, short response time, convenience operation, reproducibility and high reliability [6–8].

Recently, many studies have been focused on non-enzymatic glucose sensors based on transition metal oxides (e.g.  $\text{MnO}_2$  [9], NiO [6],  $\text{Co}_3\text{O}_4$  [10],  $\text{RuO}_2$  [11], ZnO [12] and  $\text{Fe}_2\text{O}_3$  [13]), since they are generally low in cost with high stability and high catalytic activity for glucose oxidation. Among them, copper oxide (CuO) is one of the most promising candidates due to its low toxicity, simple production, low cost, high electro-catalytic activity and its promoting effect on electron transfer rate from the transition of its redox couple during glucose oxidation [14]. Moreover, for a CuO-based glucose sensor, its sensitivity and accuracy rely upon the electro-catalytic properties of CuO, on which the glucose is directly electro-catalytically oxidised. It was found that the performance of CuO is affected by its surface characteristics which are closely related to their sizes, morphologies and crystal structure. In order to enhance performance of CuO-based glucose sensors, CuO crystals with various nanostructures, such as nanospheres [15], nanowires [16], nanosheets [17], nanourchins [18], nanofibres [19] and flower-like structures [20], have been applied in non-enzymatic glucose sensors. In the last decade, there has been some great advancement on the development of CuO-based non-enzymatic glucose sensors, however there is still scope for developing novel CuO materials using new fabrication methods.

Herein, hierarchical three-dimensional (3D) CuO materials with spindle shape (CuO spindle) were synthesised via a solvothermal method and their respective activities in glucose detection were evaluated, since hierarchical 3D CuO spindles made of numerous nanoslices contain numerous interfaces between these nanoslices.

It was found that as-prepared CuO electrode exhibits good sensing performance in terms of sensitivity, response time and a broad glucose detection range, thus making the new material a suitable candidate for non-enzymatic glucose biosensors.

## 2. Experimental

**2.1. Materials synthesis:** All chemicals were used as received without further purification. The detail procedure for preparing  $\text{Cu}(\text{OH})_2$  is as follows:  $\text{CuCl}_2$  (40 mg) was dissolved in 30 ml of ultrapure water. Then, 0.5 M NaOH solution was added dropwise into the  $\text{CuCl}_2$  solution until pH 9 was achieved. During the addition of NaOH into the solution, a blue suspension was formed. An amount of urea was dissolved into the mixture and stirred for half hour, and then the mixture was transferred into an autoclave (100 ml, Teflon-lined) and heated up at 150°C for 2 h. After cooling down to room temperature, black products were recovered by filtration, washed with deionised water several times and finally dried at 80°C for 12 h.

**2.2. Characterisation:** The crystalline structures of the sample were analysed by X-ray diffraction (XRD, Shimadzu XD-3A (Japan) goniometer, using a Cu  $K\alpha$  radiation operating at 40 kV and 35 mA). The morphologies of the catalyst were analysed using a Carl Zeiss Ultra Plus field emission scanning electron microscope (SEM), a transmission electron microscope (TEM) and a JEM-2010 electron microscope (Japan) with an acceleration voltage of 200 kV. The specific surface areas were analysed by the Brunauer–Emmett–Teller (BET) method using a Quantachrome Autosorb-1 volumetric analyser.

**2.3. Electrochemical measurements:** Electrochemical measurements were carried out using an electrochemical work station (CHI 650D potentiostat/galvanostat). A conventional three-electrode electrochemical cell was used which comprised of a platinum wire, an Ag/AgCl (saturated KCl solution), and the thin film catalyst layer mounted on a 5 mm diameter glassy carbon disc were used as counter, reference and working electrodes, respectively. The thin film was prepared as follows: 2 mg of catalyst were dispersed ultrasonically in 0.6 ml of Nafion<sup>®</sup>/ethanol (25 wt.% Nafion<sup>®</sup>). About 8  $\mu\text{l}$  of the as-prepared solution was transferred onto a glassy carbon disc and then dried in air.

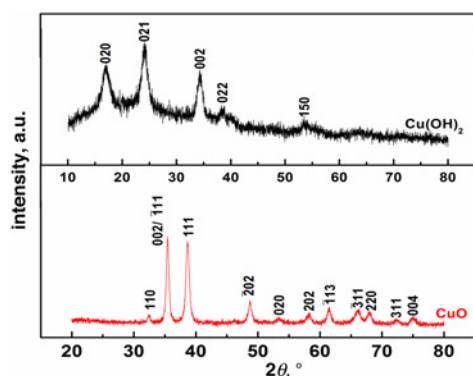


**Fig. 1** XRD patterns of the  $\text{Cu}(\text{OH})_2$  precursor and as-prepared  $\text{CuO}$  sample

**3. Results and discussion:** The crystal structure of  $\text{Cu}(\text{OH})_2$  precursor and the as-prepared  $\text{CuO}$  sample were examined by XRD. As shown in Fig. 1, the  $\text{Cu}(\text{OH})_2$  precursor exhibited typical diffraction peaks at  $2\theta$ ;  $16.9^\circ$ ,  $24.1^\circ$ ,  $34.3^\circ$ ,  $38.5^\circ$  and  $53.7^\circ$  indexed to the (020), (021), (002), (022) and (150) crystal planes of orthorhombic phase  $\text{CuO}$  (JCPDS Card No. 72-0140), respectively. In the case of  $\text{CuO}$  sample, the obtained XRD peaks were in accordance with the characteristics of monoclinic phase  $\text{CuO}$  (JCPDS Card No. 48-1548), and no evident XRD peaks of  $\text{Cu}(\text{OH})_2$  were detected, suggesting pure monoclinic  $\text{CuO}$  was formed.

Fig. 2 shows the SEM images of the  $\text{Cu}(\text{OH})_2$  precursor and  $\text{CuO}$  samples. As shown in Fig. 2a, the  $\text{Cu}(\text{OH})_2$  precursor exhibits particles of irregular shapes. Fig. 2b shows the morphology of the  $\text{CuO}$  sample made of spindle-like particles of ca.  $1\ \mu\text{m}$  in length and  $200\text{--}400\ \text{nm}$  in width. The magnified SEM image in Fig. 2c clearly shows that the individual spindles were formed by the aggregation of small nanoslices. These nanoslices are ca.  $25\ \text{nm}$  thick and connected with each other to form 3D spindle structures. TEM images shown in Figs. 2d and e confirm the presence of hierarchical structured  $\text{CuO}$  spindles made of nanoslices, suggesting that numerous interfaces between these nanoslices exist. The selected area electron diffraction (SAED) shown in Fig. 2e confirms that the  $\text{CuO}$  spindles contain many nanocrystals, but the brightness of these diffraction rings is not even, which indicates a preferential orientation of these nanocrystals. It is interesting to note that the morphologies changed from irregular-shaped particles to spindle-like particles during the transition from  $\text{Cu}(\text{OH})_2$  to  $\text{CuO}$ ; this is possibly due to a dissolution–reaction–recrystallisation process [21–23]. During the recrystallisation process, it seems that urea plays an important role in the formation of hierarchical spindle structure of the as-prepared  $\text{CuO}$ . In the absence of urea, irregular-shaped  $\text{CuO}$  particles were formed instead of spindles (as shown in Fig. 2f). Fig. 3 shows the  $\text{N}_2$  adsorption–desorption isotherms of  $\text{CuO}$  spindles and irregular-shaped  $\text{CuO}$ . The BET surface areas of  $\text{CuO}$  spindles and irregular  $\text{CuO}$  were found to be  $25.7$  and  $15.2\ \text{m}^2\text{g}^{-1}$ , respectively, implying that introducing urea into the mixture during the formation of  $\text{CuO}$  can result in higher surface area.

In addition, comparing our observations to other works, it should be noted that choosing  $\text{Cu}(\text{OH})_2$  as precursor appears to be a crucial material for the formation of hierarchical 3D  $\text{CuO}$  spindles. For example, Ghosh *et al.* [24] reported that by using the same hydrothermal method and urea as the reactant,  $\text{CuO}$  particles of irregular shapes were obtained when  $\text{Cu}(\text{NO}_3)_2$  was used as the precursor. It was also shown that the hierarchical spindle shapes cannot be obtained from other soluble copper salts (such as  $\text{CuSO}_4$  and  $\text{CuCl}_2$ ) under similar hydrothermal conditions [25–27]. These observations suggest that the copper source, namely  $\text{Cu}(\text{OH})_2$ , play a vital role in the formation of hierarchical 3D  $\text{CuO}$  spindles.

To elucidate and understand the electro-catalytic behaviour of the hierarchical 3D  $\text{CuO}$  spindles and irregular-shaped  $\text{CuO}$  in the

presence and absence of glucose in  $0.1\ \text{mol L}^{-1}$   $\text{NaOH}$ , cyclic voltammetry (CV) and chronoamperometry experiments were carried out. Fig. 4 shows three distinct CVs in the potential range of  $-0.3$  to  $+0.7\ \text{V}$  versus  $\text{Ag}/\text{AgCl}$  run at a scan rate of  $5\ \text{mV s}^{-1}$ . The CV corresponds to the voltammetric response of the  $\text{CuO}$  spindle in  $0.1\ \text{M}$   $\text{NaOH}$  only, whereas the CVs correspond to the voltammetric response of the  $\text{CuO}$  spindle (red line) and irregular-shaped  $\text{CuO}$  (blue line) in  $0.1\ \text{M}$   $\text{NaOH} + 0.1\ \text{mM}$  glucose. It can be seen that the CVs (red and blue lines) show an oxidation and a reduction peak in the potential range of  $0.1\text{--}0.7\ \text{V}$  versus  $\text{Ag}/\text{AgCl}$ , corresponding to the oxidation of  $\text{Cu}(\text{II})$  to  $\text{Cu}(\text{III})$ , and the reduction of  $\text{Cu}(\text{III})$  to  $\text{CuO}$ , respectively [28, 29]. Fig. 4 also shows that the anodic peak of  $\text{CuO}$  spindle is much higher than that of irregular-shaped  $\text{CuO}$  at ca.  $+0.40\text{--}0.50\ \text{V}$  versus  $\text{Ag}/\text{AgCl}$  in the potential range used corresponding to glucose oxidation. This observation indicates that  $\text{CuO}$  spindle is more catalytically active toward the glucose oxidation reaction than irregular-shaped  $\text{CuO}$  [18, 30].

Compared with other methods of studying glucose oxidation, amperometry is the most effective method as it offers less signal-to-noise ratio and helps achieving effective mixing of the sample solution due to increased convective mass transport to the electrode surface; in turn resulting in rapid and low electroanalyte detection. For these reasons, the amperometric method was used to investigate the electrochemical responses of the as-prepared  $\text{CuO}$  spindle electrode in the presence of  $0.1\ \text{mM}$  glucose (added dropwise) in  $0.1\ \text{M}$   $\text{NaOH}$  solution. In order to find the appropriate applied potential ( $E_{\text{app}}$ ) for the amperometric study, a series of chronoamperometric experiments on the  $\text{CuO}$  spindle electrode in  $0.1\ \text{M}$   $\text{NaOH}$  solution (only) at various potentials were performed. It was found that the chronoamperogram performed at a potential of  $+0.5\ \text{V}$  exhibited a stronger and more stable response (Fig. 5a). An applied chronoamperometric potential of  $E_{\text{app}} = +0.5\ \text{V}$  versus  $\text{Ag}/\text{AgCl}$  was then used for the rest of the investigation. Figs. 5b and e show the chronoamperometric responses of the  $\text{CuO}$  spindle and the irregular-shaped  $\text{CuO}$  with successive addition of  $0.1\ \text{mM}$  glucose in  $0.1\ \text{M}$   $\text{NaOH}$  solution at  $0.5\ \text{V}$  versus  $\text{Ag}/\text{AgCl}$ . The figure shows that as the glucose concentration is increased, a significant increase in anodic currents is observed. Chronoamperograms of the  $\text{CuO}$  spindle irregular-shaped  $\text{CuO}$  electrodes in low glucose concentration solutions were performed in order to study glucose sensitivity of the novel electrode material (Fig. 5c and the inset of Fig. 5e). It can be seen from the figure that rapid increases in currents were observed after each added glucose aliquots to the solution. The  $\text{CuO}$  spindle electrode reached 95% of the stable current just in 5 s, showing a fast current response to glucose. Calibration curves of the response (anodic) current ( $\mu\text{A}$ ) versus glucose concentration ( $\mu\text{M}$ ) for the  $\text{CuO}$  spindle and the irregular-shaped  $\text{CuO}$  were plotted as shown in Figs. 5d and f. It was found that the calibration graph of  $\text{CuO}$  spindle electrode was linear in the glucose concentration ranging from  $1\ \mu\text{M}$  to  $3\ \text{mM}$  (correlation coefficient = 0.9926) with a sensitivity value of  $2828\ \mu\text{A mM}^{-1}\ \text{cm}^{-2}$  at a signal/noise ratio of 3, which is higher than that of the irregular-shaped  $\text{CuO}$  electrode ( $1380\ \mu\text{A mM}^{-1}\ \text{cm}^{-2}$ ). Based on the BET results, the higher surface area of  $\text{CuO}$  spindle could be one of reasons resulting in its higher sensitivity compared with irregular-shape  $\text{CuO}$ . The limit of detection (LOD) of the  $\text{CuO}$  electrodes was determined using the following equation [3, 30]

$$\text{LOD} = \frac{3s_b}{m} \quad (1)$$

where  $m$  is the slope value of the calibration plot and  $s_b$  is the deviation got from ten different measurements of the blank signal. LOD is calculated to be  $0.3\ \mu\text{M}$  which is lower than the LOD obtained from irregular-shaped  $\text{CuO}$  electrode ( $0.7\ \mu\text{M}$ ).

A comparison of the  $\text{CuO}$  spindle electrode with some of the reported CO glucose biosensors is summarised in Table 1. The

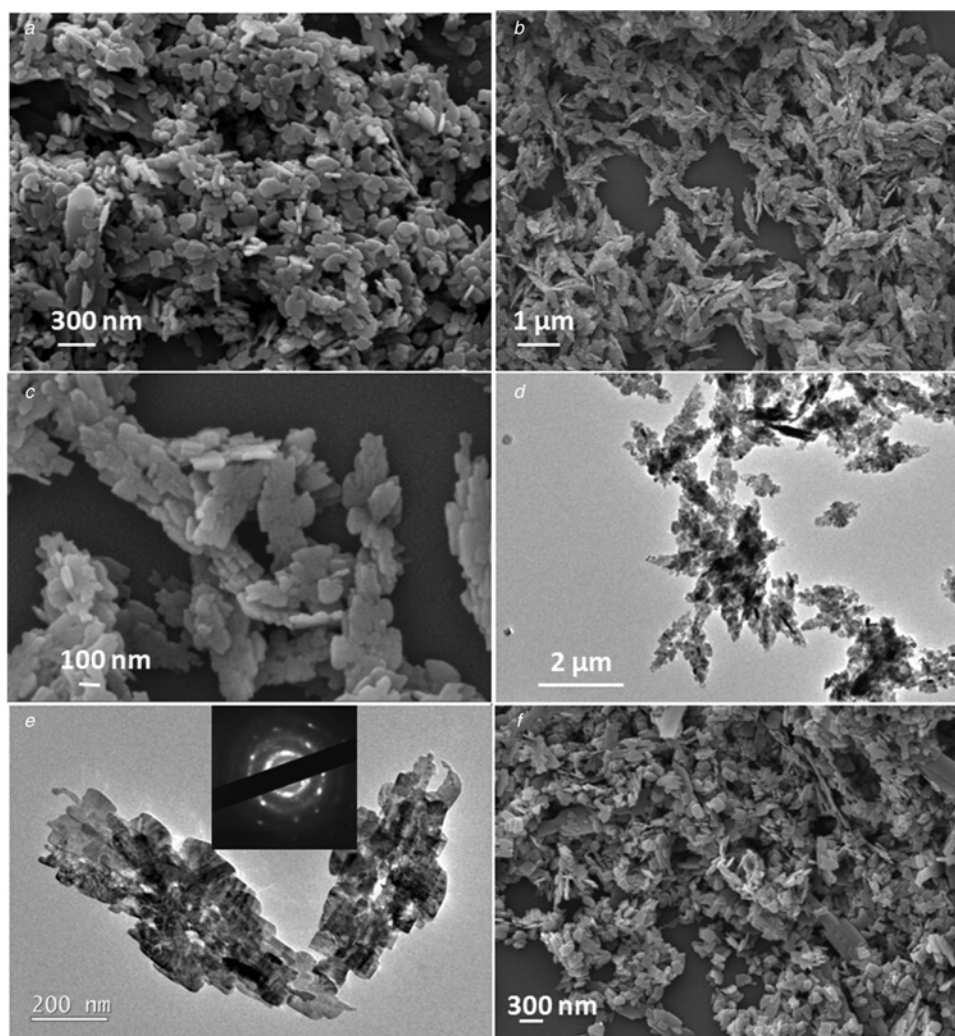


**Fig. 2** a) SEM images of  $\text{Cu}(\text{OH})_2$  precursor; b), c) SEM images of  $\text{CuO}$ ; d) TEM image of  $\text{CuO}$ ; e) TEM images and SAED pattern of  $\text{CuO}$ ; f) SEM images of  $\text{CuO}$  prepared without the presence of urea

table clearly shows that the as-prepared  $\text{CuO}$  spindle electrode exhibit acceptable sensitivity and detection limit values toward glucose when compared with other electrode materials. The high sensitivity of  $\text{CuO}$  spindle electrode may be attributed to its unique structure. As previously discussed, the  $\text{CuO}$  spindles are made of many nanoslices, among which numerous particle boundaries are formed. According to literature, these particle boundaries between the crystalline phases could act as catalytically active sites [34–36]. Thus in our conditions, it is possible that the

hierarchical structure of the as-prepared  $\text{CuO}$  spindles forms large amount of particle boundaries, which could act as catalytic active sites leading to the observed higher catalytic activity for glucose oxidation and therefore to higher glucose sensitivity.

Usually, many oxidative species, namely ascorbic acid (AA), some carbohydrate compounds and uric acid (UA), normally exist with glucose in the samples, which will further interfere with the detection of glucose. Therefore, selectivity for glucose oxidation

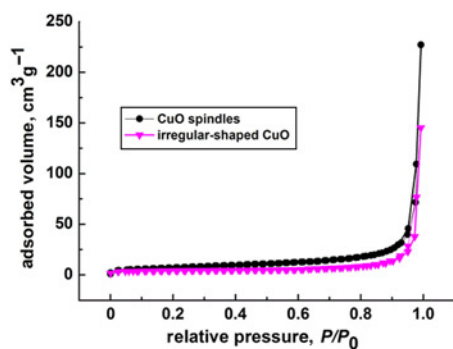


**Fig. 3**  $\text{N}_2$  adsorption–desorption isotherms of  $\text{CuO}$  spindles and irregular-shaped  $\text{CuO}$

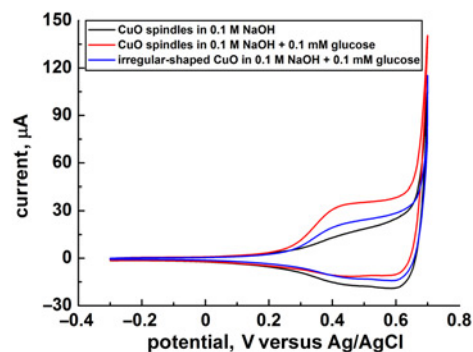


**Fig. 4** CV curves of the spindle  $\text{CuO}$  electrodes in  $0.1 \text{ M NaOH}$  and  $0.1 \text{ M NaOH} + 0.1 \text{ mM glucose}$  solution and irregular-shaped  $\text{CuO}$  electrodes in  $0.1 \text{ M NaOH} + 0.1 \text{ mM glucose}$  solution at scan rate of  $5 \text{ mV s}^{-1}$

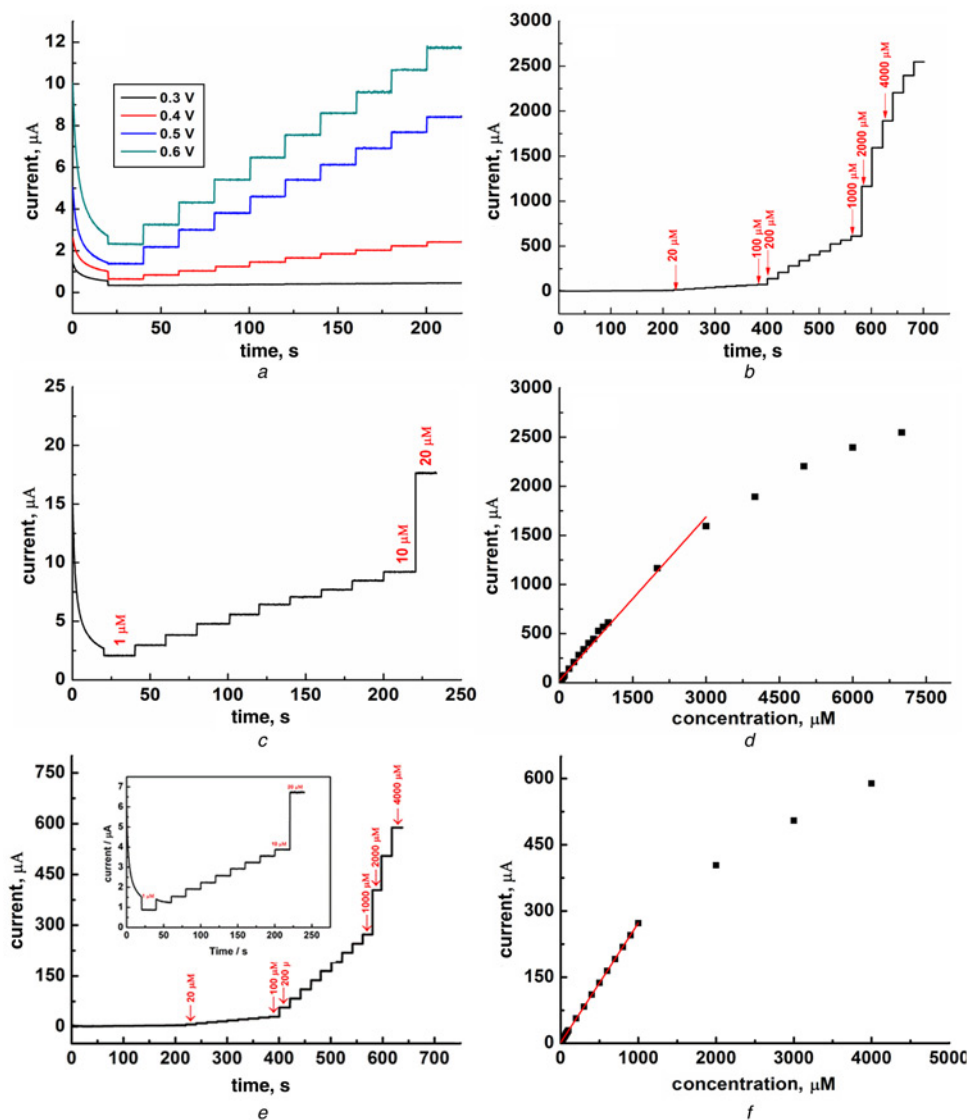


**Fig. 5** a) Amperometric response on the CuO spindle electrode with dropwise addition of 0.1 mM glucose at different potentials; b), e) Amperometric response on the CuO spindle electrode and irregular-shaped CuO electrode with successive addition of different amounts of glucose to 0.1 M NaOH at a potential of +0.5 V versus Ag/AgCl; c) Enlarged amperometric response of the CuO spindle electrode in low concentrations; d), f) Current–glucose concentration calibration curve obtained from Figs. 4b and 4f, respectively

is a key factor in practical application of glucose biosensors. According to the previous studies, normal physiological levels of glucose range between 3 and 8 mM and are at least ten times

higher than that of commonly occurring interfering species. The chronoamperometric response of the CuO spindle electrode to the stepwise addition of 1.0 mM glucose in the presence of 0.1 mM

**Table 1** Comparison of key performance for reported CuO-based electrodes in glucose detection

Electrode	Detection potential, V versus Ag/AgCl	Sensitivity, $\mu\text{A cm}^{-2} \text{mM}^{-1}$	Linear range, mM	LOD, $\mu\text{M}$	Reference
CuO spindle	0.5	2828	0.001–3	0.3	this work
irregular-shaped CuO	0.5	1380	0.001–1	0.7	this work
CuO nanowires/Cu	0.35	2217.4	0.001–18.8	0.3	[14]
CuO nanourchins	0.57	1634	0.01–5	1.97	[18]
CuO nanoparticles	0.6	2762.5	0.05–18.45	0.5	[31]
CuO nanospheres	0.60	404.53	0.05–2.55	1	[15]
CuO nanoparticles	0.40	1430	0.04–6	5	[32]
CuO nanowires	0.55	648.2	–	2	[16]
CuO nanowires/Cu	0.33	490	0.0004–2	0.049	[33]
CuO nanofibres	0.40 <sup>a</sup>	431.3	0.006–2.5	0.8	[19]
CuO nanoflowers	0.5	2657	0.01–5	1.71	[20]
dandelion-like CuO films	0.60 <sup>a</sup>	5368	0.005–1.6	1.2	[30]

<sup>a</sup>The reference electrode is saturated calomel electrode (SCE)

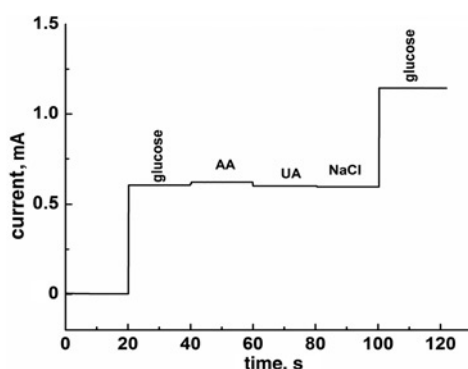


**Fig. 6** Amperometric response of the CuO electrode with continuous addition of 1.0 mM glucose and 0.1 mM interferents of AA, UA and NaCl into 0.1 M NaOH at a potential of +0.5 V (versus Ag/AgCl)

of various interferents (AA, NaCl and UA at 0.1 mM) at +0.5 V versus Ag/AgCl is shown in Fig. 6. The figure shows that an obvious current response to glucose oxidation can be observed without significant current responses to the interferents, indicating that, in our conditions, high selectivity for glucose was achieved on the CuO spindle in alkaline media. In the alkaline environment, the CuO would be negatively charged on its surface. Meanwhile, interference species such as UA and AA are also be negatively charged because of the deprotonating effect in alkaline solution [30, 31, 32, 37], and therefore would be repelled by CuO which was negatively charged, showing correspondingly low signals. It was reported that the method used in this Letter can be used in blood and urine samples for glucose detection. For instance, serum sample was also added into 0.1 M NaOH solution for testing glucose oxidation. The obtained results from this method are consistent with the results from medical instrument, Beckman [38, 39].

**4. Conclusion:** Hierarchical 3D CuO spindles made of numerous nanoslices were synthesised via a hydrothermal method. The as-prepared CuO spindle electrode showed good sensing performance in terms of response time (ca. 3 s) and sensitivity (ca.  $3000 \mu\text{A mM}^{-1} \text{cm}^{-2}$ ) of detecting glucose with a broad detection range of 0.001–3 mM. Since the as-prepared CuO spindles consisted of numerous particle boundaries between the nanoslices, it was observed that they could act as catalytic active sites for the glucose oxidation, in turn leading to lower detection limits and higher sensitivity (when compared with other CuO-based electrodes). The CuO spindle electrode also demonstrated excellent selectivity. The high sensitivity and selectivity makes the as-prepared CuO spindle electrode a promising non-enzymatic glucose biosensor for practical applications.

**5. Acknowledgments:** The authors thank the National Natural Science Foundation of China (grant nos. 21363022 and 51362027) and JCYJ20140418095735600 for financially supporting this work.

## 6 References

- [1] Mijowska E., Onyszko M., Urbas K., *ET AL.*: 'Palladium nanoparticles deposited on graphene and its electrochemical performance for glucose sensing', *Appl. Surf. Sci.*, 2015, **355**, pp. 587–592
- [2] Li H., Li J., Chen D., *ET AL.*: 'Dual-functional cubic cuprous oxide for non-enzymatic and oxygen-sensitive photoelectrochemical sensing of glucose', *Sens. Actuators B, Chem.*, 2015, **220**, pp. 441–447
- [3] Yang J., Cho M., Lee Y.: 'Synthesis of hierarchical nicoo hollow nanorods via sacrificial-template accelerate hydrolysis for electrochemical glucose oxidation', *Biosens. Bioelectron.*, 2015, **75**, pp. 15–22
- [4] Shahnava Z., Woi P.M., Alias Y.: 'A hydrothermally prepared reduced graphene oxide-supported copper ferrite hybrid for glucose sensing', *Ceram. Int.*, 2015, **41**, (10), pp. 12710–12716
- [5] Yu Z., Li H., Zhang X., *ET AL.*: 'Facile synthesis of nico2o4@Polyaniline core-shell nanocomposite for sensitive determination of glucose', *Biosens. Bioelectron.*, 2016, **75**, pp. 161–165
- [6] Veeramani V., Madhu R., Chen S.-M., *ET AL.*: 'Heteroatom-enriched porous carbon/nickel oxide nanocomposites as enzyme-free highly sensitive sensors for detection of glucose', *Sens. Actuators B, Chem.*, 2015, **221**, pp. 1384–1390
- [7] Basiruddin S.K., Swain S.K.: 'Phenylboronic acid functionalized reduced graphene oxide based fluorescence nano sensor for glucose sensing', *Mater. Sci. Eng. C, Mater. Biol. Appl.*, 2016, **58**, pp. 103–109
- [8] Sivasakthi P., Ramesh Babu G.N., Chandrasekaran M.: 'Pulse electrodeposited nickel-indium tin oxide nanocomposite as an electrocatalyst for non-enzymatic glucose sensing', *Mater. Sci. Eng. C, Mater. Biol. Appl.*, 2016, **58**, pp. 782–789
- [9] Yang S., Liu L., Wang G., *ET AL.*: 'One-pot synthesis of Mn3o4 nanoparticles decorated with nitrogen-doped reduced graphene oxide for sensitive nonenzymatic glucose sensing', *J. Electroanal. Chem.*, 2015, **755**, pp. 15–21
- [10] Guo C., Zhang X., Huo H., *ET AL.*: 'Co3o4 microspheres with free-standing nanofibers for high performance non-enzymatic glucose sensor', *Analyst*, 2013, **138**, (22), pp. 6727–6731
- [11] Tehrani R.M., Ab Ghani S.: 'Mwcnt-ruthenium oxide composite paste electrode as non-enzymatic glucose sensor', *Biosens. Bioelectron.*, 2012, **38**, (1), pp. 278–283
- [12] Singh K., Umar A., Kumar A., *ET AL.*: 'Non-enzymatic glucose sensor based on well-crystallized ZnO nanoparticles', *Sci. Adv. Mater.*, 2012, **4**, (9), pp. 994–1000
- [13] Cao X., Wang N.: 'A novel non-enzymatic glucose sensor modified with Fe<sub>2</sub>O<sub>3</sub> nanowire arrays', *Analyst*, 2011, **136**, (20), pp. 4241–4246
- [14] Li Z., Chen Y., Xin Y., *ET AL.*: 'Sensitive electrochemical nonenzymatic glucose sensing based on anodized CuO nanowires on three-dimensional porous copper foam', *Sci. Rep.*, 2015, **5**, p. 16115
- [15] Reitz E., Jia W., Gentile M., *ET AL.*: 'CuO nanospheres based nonenzymatic glucose sensor', *Electroanalysis*, 2008, **20**, (22), pp. 2482–2486
- [16] Wang X., Hu C., Liu H., *ET AL.*: 'Synthesis of CuO nanostructures and their application for nonenzymatic glucose sensing', *Sens. Actuators B, Chem.*, 2010, **144**, (1), pp. 220–225
- [17] Ibupoto Z., Khun K., Beni V., *ET AL.*: 'Synthesis of novel CuO nanosheets and their non-enzymatic glucose sensing applications', *Sensors*, 2013, **13**, (6), pp. 7926–7938
- [18] Sun S., Zhang X., Sun Y., *ET AL.*: 'A facile strategy for the synthesis of hierarchical CuO nanourchins and their application as non-enzymatic glucose sensors', *RSC Adv.*, 2013, **3**, (33), pp. 13712–13719
- [19] Wang W., Zhang L., Tong S., *ET AL.*: 'Three-dimensional network films of electrospun copper oxide nanofibers for glucose determination', *Biosens. Bioelectron.*, 2009, **25**, (4), pp. 708–714
- [20] Sun S., Zhang X., Sun Y., *ET AL.*: 'Hierarchical CuO nanoflowers: water-required synthesis and their application in a nonenzymatic glucose biosensor', *Phys. Chem. Chem. Phys.*, 2013, **15**, (26), p. 10904
- [21] Chen L., Xiong Q., Li W., *ET AL.*: 'A solvothermal transformation of A-Fe<sub>2</sub>O<sub>3</sub> nanocrystals to Fe<sub>3</sub>O<sub>4</sub> polyhedrons', *CrystEngComm*, 2015, **17**, pp. 8602–8606
- [22] Chen L., Yang X., Chen J., *ET AL.*: 'Continuous shape- and spectroscopy-tuning of hematite nanocrystals', *Inorg. Chem.*, 2010, **49**, (18), pp. 8411–8420
- [23] Peng Q., Dong Y., Deng Z., *ET AL.*: 'Selective synthesis and magnetic properties of A-Mnse and Mnse2 uniform microcrystals', *J. Phys. Chem. B*, 2002, **106**, (36), pp. 9261–9265
- [24] Ghosh S., Roy M., Naskar M.K.: 'Template-free synthesis of mesoporous single-crystal CuO particles with dumbbell-shaped morphology', *Mater. Lett.*, 2014, **132**, pp. 98–101
- [25] Yang C., Wang J., Xiao F., *ET AL.*: 'Microwave hydrothermal disassembly for evolution from CuO dendrites to nanosheets and their applications in catalysis and photo-catalysis', *Powder Technol.*, 2014, **264**, pp. 36–42
- [26] Moosavifard S.E., Shamsi J., Fani S., *ET AL.*: 'Facile synthesis of hierarchical CuO nanorod arrays on carbon nanofibers for high-performance supercapacitors', *Ceram. Int.*, 2014, **40**, (10), pp. 15973–15979
- [27] Yuan Y.F., Pei Y.B., Fang J., *ET AL.*: 'Sponge-like mesoporous cuo ribbon clusters as high-performance anode material for lithium-ion batteries', *Mater. Lett.*, 2013, **91**, pp. 279–282

- [28] Ma Y., Wang H., Julian K., *ET AL.*: 'Control of CuO nanocrystal morphology from ultrathin "willow-leaf" to "flower-shaped" for increased hydrazine oxidation activity', *J. Power Sources*, 2015, **300**, pp. 344–350
- [29] Ma Y., Li H., Wang R., *ET AL.*: 'Ultrathin willow-like CuO nanoflakes as an efficient catalyst for electro-oxidation of hydrazine', *J. Power Sources*, 2015, **289**, pp. 22–25
- [30] Li K., Fan G., Yang L., *ET AL.*: 'Novel ultrasensitive non-enzymatic glucose sensors based on controlled flower-like CuO hierarchical films', *Sens. Actuators B, Chem.*, 2014, **199**, pp. 175–182
- [31] Ahmad R., Vaseem M., Tripathy N., *ET AL.*: 'Wide linear-range detecting nonenzymatic glucose biosensor based on CuO nanoparticles inkjet-printed on electrodes', *Anal. Chem.*, 2013, **85**, (21), pp. 10448–10454
- [32] Huang F., Zhong Y., Chen J., *ET AL.*: 'Nonenzymatic glucose sensor based on three different CuO nanomaterials', *Anal. Methods*, 2013, **5**, (12), pp. 3050–3050
- [33] Zhuang Z., Su X., Yuan H., *ET AL.*: 'An improved sensitivity non-enzymatic glucose sensor based on a CuO nanowire modified Cu electrode', *Analyst*, 2008, **133**, (1), pp. 126–132
- [34] Maillard F., Schreier S., Hanzlik M., *ET AL.*: 'Influence of particle agglomeration on the catalytic activity of carbon-supported Pt nanoparticles in Co monolayer oxidation', *Phys. Chem. Chem. Phys.*, 2005, **7**, pp. 385–393
- [35] Zhang J., Xu Y., Zhang B.: 'Facile synthesis of 3d Pd-P nanoparticle networks with enhanced electrocatalytic performance towards formic acid electrooxidation', *Chem. Commun.*, 2014, **50**, pp. 13451–13453
- [36] Wang H., Liu Z., Ma Y., *ET AL.*: 'Synthesis of carbon-supported PdSn-SnO<sub>2</sub> nanoparticles with different degrees of interfacial contact and enhanced catalytic activities for formic acid oxidation', *Phys. Chem. Chem. Phys.*, 2013, **15**, (33), pp. 13999–14005
- [37] Sun S., Zhang X., Sun Y., *ET AL.*: 'Facile water-assisted synthesis of cupric oxide nanourchins and their application as nonenzymatic glucose biosensor', *ACS Appl. Mater. Interfaces*, 2013, **5**, (10), pp. 4429–4437
- [38] Yang J., Jiang L., Zhang W., *ET AL.*: 'A highly sensitive non-enzymatic glucose sensor based on a simple two-step electrodeposition of cupric oxide (CuO) nanoparticles onto multi-walled carbon nanotube arrays', *Talanta*, 2010, **82**, pp. 25–33
- [39] Jian L., Zhou C., Xing R., *ET AL.*: 'Synthesis of graphene oxide based CuO nanoparticles composite electrode for highly enhanced nonenzymatic glucose detection', *Appl. Mater. Interfaces*, 2013, **5**, pp. 12928–12934